blood®
Regular Article

HEMATOPOIESIS AND STEM CELLS

A human SIRPA knock-in xenograft mouse model to study human hematopoietic and cancer stem cells

Fumiaki Jinnouchi,[1] Takuji Yamauchi,[1,2] Ayano Yurino,[1] Takuya Nunomura,[1] Michitaka Nakano,[1] Chika Iwamoto,[3] Teppei Obara,[1] Kohta Miyawaki,[1,4] Yoshikane Kikushige,[1] Koji Kato,[1] Takahiro Maeda,[2] Toshihiro Miyamoto,[1] Eishi Baba,[1] Koichi Akashi,[1] and Katsuto Takenaka[5]

[1]Department of Medicine and Biosystemic Science, Kyushu University Graduate School of Medical Sciences, Fukuoka, Japan; [2]Center for Cellular and Molecular Medicine, Kyushu University Hospital, Fukuoka, Japan; [3]Department of Surgery and Oncology, Kyushu University Graduate School of Medical Sciences, Fukuoka, Japan; [4]Department of Pathology, Kurume University School of Medicine, Kurume, Japan; and [5]Hematology, Clinical Immunology, and Infectious Diseases, Ehime University Graduate School of Medicine, Ehime, Japan

KEY POINTS

- **Human SIRPA knock-in mice should be an ideal basic xenograft model to analyze hematopoiesis, leukemogenesis, and tumorigenesis in humans.**

In human-to-mouse xenogeneic transplantation, polymorphisms of signal-regulatory protein α (SIRPA) that decide their binding affinity for human CD47 are critical for engraftment efficiency of human cells. In this study, we generated a new C57BL/6.*Rag2*^{null}*Il2rg*^{null} (BRG) mouse line with *Sirpa*$^{human/human}$ (BRGS^{human}) mice, in which mouse *Sirpa* was replaced by human *SIRPA* encompassing all 8 exons. Macrophages from C57BL/6 mice harboring *Sirpa*$^{human/human}$ had a significantly stronger affinity for human CD47 than those harboring *Sirpa*$^{NOD/NOD}$ and did not show detectable phagocytosis against human hematopoietic stem cells. In turn, *Sirpa*$^{human/human}$ macrophages had a moderate affinity for mouse CD47, and BRGS^{human} mice did not exhibit the blood cytopenia that was seen in *Sirpa*$^{-/-}$ mice. In human to mouse xenograft experiments, BRGS^{human} mice showed significantly greater engraftment and maintenance of human hematopoiesis with a high level of myeloid reconstitution, as well as improved reconstitution in peripheral tissues, compared with BRG mice harboring *Sirpa*$^{NOD/NOD}$ (BRGS^{NOD}). BRGS^{human} mice also showed significantly enhanced engraftment and growth of acute myeloid leukemia and subcutaneously transplanted human colon cancer cells compared with BRGS^{NOD} mice. BRGS^{human} mice should be a useful basic line for establishing a more authentic xenotransplantation model to study normal and malignant human stem cells. (*Blood*. 2020;135(19):1661-1672)

Introduction

Xenogeneic transplantation using immunodeficient mouse models is an established method to analyze human hematopoiesis and tumorigenesis.[1-3] Over the decades, extensive progress has been made in establishing mouse lines that are capable of efficient engraftment and growth of human hematopoietic stem cells (HSCs) or cancer stem cells. These xenotransplantation models are necessary to develop translational cancer research.[4]

Successful xenotransplantation can be achieved primarily through prevention of human graft rejection. To deplete T and B cells from recipient mice, the *scid* mutation in *Prkdc*[5-7] or disruption of the recombination activating gene 1 and 2 (*Rag1* and *Rag2*)[8-10] have been introduced. In addition, to deplete NK cells or their functions, the interleukin-2 receptor common γ chain subunit (*Il2rg*) or *B2m* was disrupted.[11-13] It has also been empirically shown that mice with the nonobese diabetic (NOD) or BALB/c genetic background exhibit efficient human-to-mouse xenotransplantation of hematopoiesis.[14] Accordingly, immunodeficient mice on a NOD or BALB/c background, including NOD-*scid Il2rg*^{null},[12,13] NOD.*Rag1*^{null}*Il2rg*^{null} (NOD-RG),[15] and BALB/c.*Rag1/2*^{null}*Il2rg*^{null} (BALB-RG)[14-16] strains, have been gold standard mouse models for xenogeneic transplantation studies.

We have reported that the strain-specific genetic determinant of human hematopoiesis engraftment was a polymorphism of the signal-regulatory protein α (*Sirpa*) gene.[17-19] SIRPA is a transmembrane protein that is expressed on macrophages and binds its ligand, CD47, which is ubiquitously expressed.[20] The binding of CD47 by SIRPA mediates inhibitory signals for macrophages to prevent autophagocytic activities: the so-called "don't eat me" signaling.[20-22] This binding is species specific; in most mouse strains, mouse SIRPA cannot recognize human CD47, resulting in activation of mouse macrophages and rejection of grafted human tissues.[17,18]

In normal hematopoiesis, CD47-SIRPA signaling is necessary to maintain homeostasis, because homozygous *Sirpa*-knockout (*Sirpa*$^{-/-}$) mice developed anemia and thrombocytopenia, presumably as a result of enhanced blood cell clearance from the circulation[23] and/or malformation of the hematopoietic niche.[24] Interestingly, the mouse SIRPA immunoglobulin variable (IgV)

domain is highly polymorphic, and the unique SIRPA IgV domains of NOD and BALB/c mice confer an enhanced affinity for human CD47.[17] The binding affinity of recipient SIRPA to human CD47 should be 1 of the critical factors that determines the efficiency of human-to-mouse xenotransplantation. We have shown that NOD SIRPA has the strongest affinity to human CD47, whereas BALB/c SIRPA has an intermediate affinity, and C57BL/6 (B6) SIRPA has no affinity; the affinity levels appeared to correlate with reconstitution levels of human hematopoiesis after xenotransplantation.[17,25] This was confirmed by our study showing that the replacement of B6 *Sirpa* with NOD *Sirpa* in the C57BL/6.*Rag2*^{null}*Il2rg*^{null} (BRG) mouse greatly improved the efficiency of human hematopoiesis engraftment.[19] The BRG-*Sirpa*$^{NOD/NOD}$ (BRGS^{NOD}) mice efficiently supported human hematopoiesis that was equal to or even better than NOD-RG mice,[19] whose efficiency had been reported to be nearly equivalent to NOD.Cg-*Prkdc*^{scid} *Il2rg*^{tm1Wjl}/SzJ (NSG) mice.[14,15]

Several studies have also shown that the enforced expression of human SIRPA can enhance human hematopoiesis in immunodeficient mice. The introduction of a bacterial artificial chromosome (BAC) minigene that encompasses the entire human *SIRPA* gene into 129×BALB/c.*Rag2*^{null}*Il2rg*^{null} (129.BALB-RG) mice significantly improved human hematopoiesis to a level comparable to that of NSG mice.[26] In another study, the extracellular domain of human *SIRPA* (exons 2-4) was knocked into the 129.BALB-RG strain to form chimeric human/mouse *Sirpa*, preserving the intracellular portion of mouse *Sirpa*.[27] 129.BALB-RG mice with a heterozygous human *SIRPA* knock-in allele could reconstitute human hematopoiesis comparable to NSG mice; interestingly, homozygous mice exhibited a significantly lower level of human hematopoiesis. This result was interpreted that, like the phenotype of *Sirpa*$^{-/-}$ mice,[24] SIRPA signal–dependent osteogenic differentiation for forming hematopoietic niches in the bone might be impaired in homozygous *SIRPA* knock-in mice, presumably because the chimeric SIRPA did not recognize mouse CD47.

In the present study, we generated B6 mice with a knock-in allele for full-length human *SIRPA* encompassing all 8 exons (B6-*Sirpa*$^{hu/hu}$). In vitro measurement of affinity for human CD47 demonstrated that B6-*Sirpa*$^{hu/hu}$ macrophages had the greatest affinity, and heterozygous B6-*Sirpa*$^{hu/W}$ and B6-*Sirpa*$^{NOD/NOD}$ macrophages exhibited intermediate affinity. Strikingly, B6-*Sirpa*$^{hu/hu}$ macrophages showed a moderate level of affinity for mouse CD47. We then established the BRG mouse line harboring *Sirpa*$^{hu/hu}$ (BRGS^{human}). BRGS^{human} mice had a long lifespan and did not develop anemia or thrombocytopenia. Human hematopoietic multilineage reconstitution after transplantation of human CB was significantly improved in BRGS^{human} mice, which was further emphasized in the peripheral blood and spleen. In addition, BRGS^{human} mice showed better engraftment potential for human acute myeloid leukemia (AML) cells and human colorectal cancer (CRC) cells compared with BRGS^{NOD} mice. Thus, the BRGS^{human} mouse should be a useful xenograft model to analyze normal and malignant hematopoiesis, as well as tumorigenesis, in humans.

Materials and methods

Mice

C57BL/6J, B6.Cg-*Rag2*$^{tm1.1Cgn}$/J, B6.129S4-*Il2rg*^{tm1Wjl}/J, and NSG mice were purchased from The Jackson Laboratory. We established a new human *SIRPA* knock-in mouse line using the targeting vector, including full-length human *SIRPA* coding sequence with the BGHpA sequence (supplemental Figure 1A, available on the *Blood* Web site), which resulted in a B6 mouse line with human *SIRPA* knocked into the mouse *Sirpa* loci. We intercrossed these strains by conventional breeding to obtain BRGS^{human} mice. BRGS^{NOD} mice were developed in our laboratory (at Department of Medicine and Biosystemic Science, Kyushu University Graduate School of Medical Sciences) as previously described.[19] *Rag2*, *Il2rg*, and *Sirpa* genes were genotyped by direct sequencing after PCR amplification to identify the genotype of BRGS^{human} mice. Primer sequences are described in supplemental Table 1. All mice were bred and maintained under specific pathogen–free conditions at the Kyushu University Animal Facility. All experiments were conducted following the guidelines of the institutional animal committee of Kyushu University.

Determination of the irradiation dose

BRG and BRGS^{NOD} mice exhibit more tolerance for irradiation than do NOG/NSG mice, which are highly radiosensitive, presumably because of the *scid* mutation. To determine the irradiation dose for BRGS^{human} mice, 6- to 8-week-old BRGS^{human} mice were irradiated with 400 to 640 cGy and monitored for 8 weeks (supplemental Figure 1B). Early deaths were observed in the mouse group irradiated with >620 cGy, whereas mice irradiated with 450 to 600 cGy were still alive at the end of the 8 weeks. Thus, as preconditioning for xenotransplantation experiments, BRGS^{human} mice were irradiated with 600 cGy, and BRGS^{NOD}, BRG, and NSG mice were irradiated with 550 cGy, 670 cGy, and 220 cGy, respectively, based on previous studies.[11,13,19]

Xenotransplantation of human cells into immunodeficient mice

Lineage (Lin)-depleted CB cells were obtained using magnetic beads (Lineage Cell Depletion Kit; Miltenyi Biotec), and Lin$^-$CD34$^+$CD38$^-$ CB cells were sorted using a FACSAria II or III (BD Biosciences). It has been shown that human cell chimerism after xenotransplantation is higher in female mice than in male mice.[19,28] As shown in supplemental Figure 2, this was also the case for BRGS^{human} mice, in terms of human cell chimerism after transplantation, for the bone marrow and the periphery. It has also been shown that, with regard to xenotransplantation using adult mice, intrafemoral injection was more efficient than IV injection.[29] As shown in supplemental Figure 3, intrafemoral injection was significantly superior to IV injection in BRGS^{NOD} mice. Based on these data, transplantation was restricted to female recipients using intrafemoral injection to exclude those variables.

To reconstitute human hematopoiesis in mice, Lin$^-$CD34$^+$CD38$^-$ CB cells (5×10^3 per mouse) were injected into the right femur of 6- to 8-week-old irradiated mice, as previously described.[19,28] Mice were euthanized, and samples were analyzed 10 to 12 weeks or 20 to 24 weeks after transplantation. Human CB cells were collected during normal full-term deliveries, after obtaining informed consent and in accordance with the Declaration of Helsinki, and were provided by the Japanese Red Cross Kyushu Cord Blood Bank.

To assess the reconstitution capability of human cancer cells, xenotransplantation of AML and CRC cells was performed. A

total of 1×10^6 $CD33^+CD45^{lo}$ or $CD34^+$ leukemia cells purified from AML patients was transplanted into irradiated mice. The DLD-1 cell line was purchased from American Type Culture Collection and injected subcutaneously with Matrigel (BD Biosciences), as previously described.[30] For in vivo limiting dilution analysis, 40, 200, or 1000 DLD-1 cells were injected into $BRGS^{human}$ and $BRGS^{NOD}$ mice (n = 6 each). To establish a patient-derived CRC xenograft model, CRC cells were obtained as surgical specimens and injected subcutaneously with Matrigel into $BRGS^{NOD}$ mice. Engrafted tumor cells were collected, and 1×10^5 engrafted CRC cells were injected into $BRGS^{human}$ and $BRGS^{NOD}$ mice (n = 6 each). All animal experiments were performed in accordance with the Institutional Animal Welfare Guidelines of Kyushu University. Clinical samples were collected after written informed consent was obtained from patients at Kyushu University Hospital. The study protocol was approved by the Institutional Review Board of Kyushu University Hospital.

Flow cytometric analysis of mouse and human hematopoietic cells

For the analyses of mouse T, B, and natural killer (NK) cells, mouse peripheral blood cells were stained with fluorescein isothiocyanate (FITC)-conjugated anti-CD19, phycoerythrin (PE)-conjugated anti-CD3, allophycocyanin (APC)-conjugated anti-NK1.1, and Pacific Blue–conjugated anti–Gr-1 antibodies. To confirm expression of SIRPA at the protein level, mouse macrophages were stained with FITC-conjugated anti-mouse CD11b, PE-conjugated anti-mouse SIRPA, and APC-conjugated anti-human SIRPA antibodies. Sorting of the $Lin^-CD34^+CD38^-$ subfraction in human CB samples was accomplished by staining with FITC-conjugated anti-CD34 antibodies, BV421-conjugated anti-CD38 antibodies, and a PerCP-Cy5.5–conjugated lineage cocktail including anti-human CD3, CD4, CD8, CD10, CD11b, CD14, CD19, CD20, CD56, and CD235ab antibodies. For the analysis and sorting of human cells after xenogeneic transplantation, we used a combination of FITC-conjugated anti-human CD33 or CD34, PE-conjugated anti-human NKp46 or CD10, PE-Cy7–conjugated anti-human CD19 or CD20, APC-conjugated anti-human CD3 or IgM, APC-Cy7–conjugated anti-human CD45, Pacific Blue–conjugated anti-mouse CD45 or anti-human CD19, and PerCP-Cy5.5–conjugated anti-mouse TER-119 antibodies. Fluorochrome-conjugated antibodies used for flow cytometric analysis are listed in supplemental Table 2. The cells were analyzed and sorted with a FACSAria II or III cell sorter.

SIRPA-CD47 binding assay

Mouse macrophages were obtained by peritoneal lavage, as described previously.[17,21] The binding of SIRPA and CD47 was assessed by flow cytometry and a peroxidase activity assay, as detailed previously.[17] For the analysis using flow cytometry, mouse macrophages were stained with FITC-conjugated CD11b, PE-conjugated anti-mouse SIRPA, and biotinylated human CD47-Fc plus APC-conjugated streptavidin. The cells were analyzed with a FACSAria III cell sorter. For the peroxidase activity assay, mouse macrophages were incubated at 37°C in a 96-well plate in the presence of increasing concentrations of purified human or mouse CD47-Fc fusion protein and then incubated at 4°C with horseradish peroxidase–conjugated goat polyclonal antibody specific for the Fcγ fragment of human IgG (Jackson ImmunoResearch), followed by a peroxidase assay. Human or mouse CD47-Fc fusion protein binding was determined by absorbance at 490 nm on a microplate reader. Nonlinear regression analysis was performed to calculate dissociation constant (Kd) and maximal binding capacity (Bmax) using the KaleidaGraph analysis program.

In vitro mouse macrophage phagocytosis assays for human HSC populations

Phagocytic activity of mouse macrophages against the human $CD34^+CD38^-$ population was evaluated in vitro, as described.[17] In brief, mouse peritoneal-derived macrophages were incubated with mouse interferon-γ (100 ng/mL; R&D Systems) and lipopolysaccharide (0.3 μg/μL) and then opsonized human CB-derived HSCs were added. After 2 hours of incubation, the phagocytic index was calculated using the following formula: phagocytic index = number of ingested cells/(number of macrophages/100). At least 200 macrophages were counted per well.

Statistical analysis

The Student *t* test was used for single comparisons, and 1-way analysis of variance, followed by Tukey's HSD (honestly significant difference) test was used for multiple comparisons. All statistical analyses were performed using JMP software (version 13.0; SAS Institute), and P values $< .05$ were considered statistically significant. The Mantel-Cox log-rank test was used to obtain survival curves.

Results

Sirpa$^{hu/hu}$ macrophages recognize human CD47 more strongly than do *Sirpa*$^{NOD/NOD}$ macrophages, preventing engulfment of human HSCs

The function of mouse and human SIRPA was tested in peritoneal macrophages from B6 mice with wild-type mouse *Sirpa* (*Sirpa*$^{W/W}$), B6 mice with homozygous NOD-type mouse *Sirpa* (*Sirpa*$^{NOD/NOD}$), and B6 mice with heterozygous or homozygous knock-in human *SIRPA* (*Sirpa*$^{hu/W}$ or *Sirpa*$^{hu/hu}$, respectively). As shown in Figure 1A, macrophages from *Sirpa*$^{W/W}$ mice expressed only mouse SIRPA, whereas those from *Sirpa*$^{hu/hu}$ mice expressed human SIRPA but not mouse SIRPA, demonstrating that mouse and human SIRPA were successfully replaced in the *Sirpa*$^{hu/hu}$ mouse.

Figure 1B shows dose-response curves for the interaction between SIRPA on macrophages and human CD47-Fc protein, as determined by a SIRPA-CD47 binding assay. *Sirpa*$^{hu/hu}$ macrophages showed the strongest binding with human CD47-Fc protein (Bmax, 3.02), whereas *Sirpa*$^{hu/W}$ and *Sirpa*$^{NOD/NOD}$ macrophages had an intermediate level of binding (Bmax, 1.69 and 1.80, respectively), and *Sirpa*$^{W/W}$ macrophages only showed nonspecific binding. The amount of CD47-Fc protein capable of binding to SIRPA expressed on macrophages from each strain was measured by flow cytometry (Figure 1C). Differences in the saturated amount of human CD47 on the surface of each type of macrophage corresponded to their affinity in the binding assay (Figure 1B), confirming that the affinity of *Sirpa*$^{hu/hu}$ macrophages for human CD47 is superior to that of *Sirpa*$^{NOD/NOD}$ macrophages.

To test human CD47-SIRPA signaling, we measured the phagocytic activity of macrophages purified from each mouse strain toward an opsonized human $Lin^-CD34^+CD38^-$ HSC

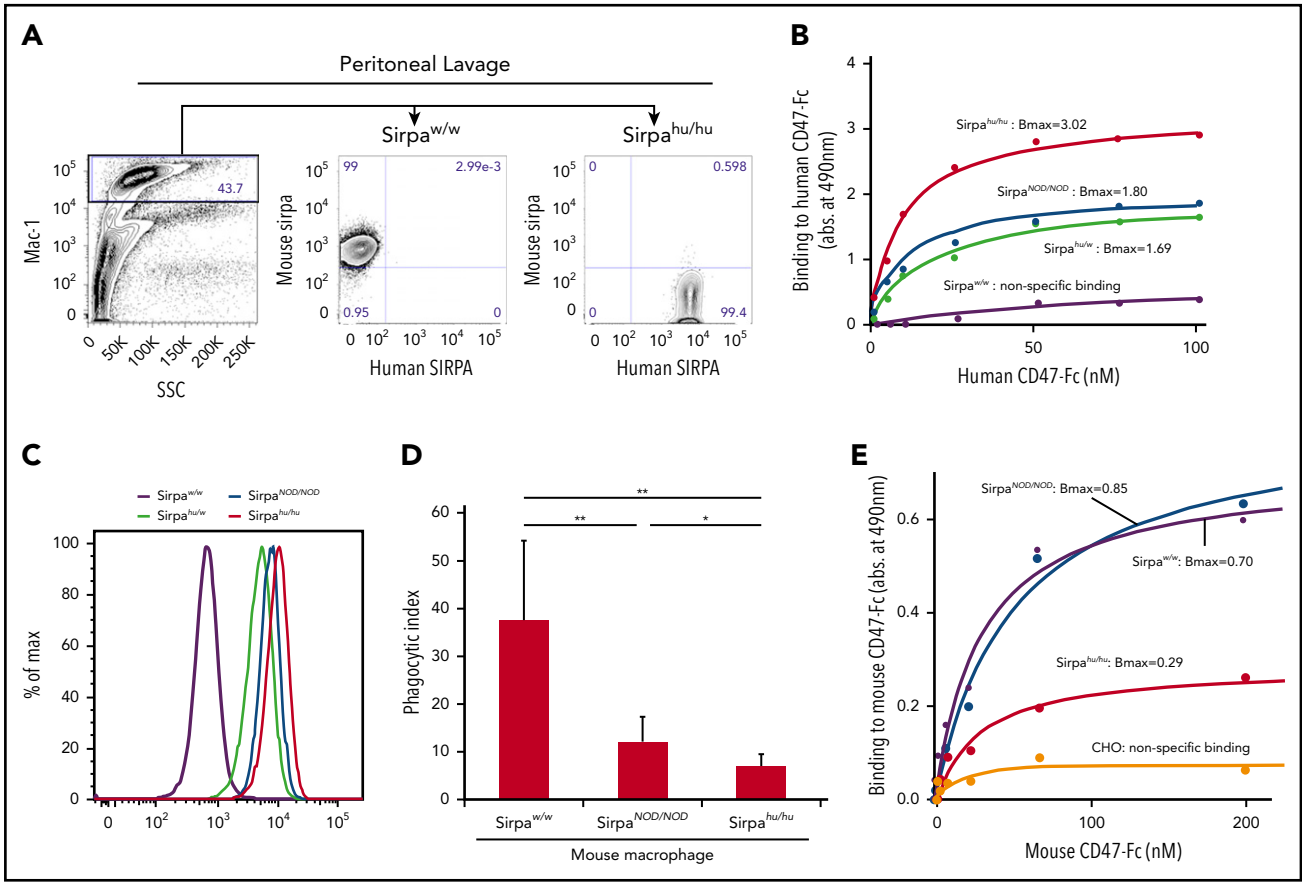

Figure 1. *Sirpa*$^{hu/hu}$ macrophages bind human CD47 more strongly than do *Sirpa*$^{NOD/NOD}$ macrophages, and they also recognize mouse CD47. (A) Representative flow cytometric plots of peritoneal lavage in B6-*Sirpa*$^{W/W}$ and B6-*Sirpa*$^{hu/hu}$ mice. Mac-1$^+$ peritoneal macrophages from B6-*Sirpa*$^{hu/hu}$ mice express human SIRPA but not mouse SIRPA. (B) Results of dose-dependent binding assays of human CD47-Fc fusion protein to B6-*Sirpa*$^{W/W}$, B6-*Sirpa*$^{NOD/NOD}$, B6-*Sirpa*$^{hu/W}$, and B6-*Sirpa*$^{hu/hu}$ mouse macrophages. *Sirpa*$^{hu/hu}$ macrophages had the strongest binding affinity for human CD47 (Bmax, 3.02 ± 0.19), and *Sirpa*$^{hu/W}$ or *Sirpa*$^{NOD/NOD}$ macrophages had intermediate levels of affinity (Bmax, 1.69 ± 0.23 and 1.80 ± 0.06, respectively), whereas *Sirpa*$^{W/W}$ macrophages did not bind to human CD47. (C) Flow cytometric analysis of macrophage binding to human CD47-Fc fusion. (D) Phagocytosis of opsonized human Lin$^-$CD34$^+$CD38$^-$ HSCs by mouse macrophages. The phagocytic index was calculated as the number of engulfed human cells per 100 macrophages. Data are mean ± standard deviation. (E) Dose-dependent binding of mouse CD47-Fc to macrophages. *Sirpa*$^{hu/hu}$ macrophages had moderate binding affinity for mouse CD47 (Bmax, 0.29 ± 0.02). Chinese hamster ovary (CHO) cells that did not express mouse or human SIRPA were used as a negative control. *$P < .05$, **$P < .01$. SSC, side scatter.

population (Figure 1D). *Sirpa*$^{W/W}$ macrophages had strong phagocytic activity against the human HSC population, whereas *Sirpa*$^{NOD/NOD}$ macrophages showed significantly reduced phagocytic activity. Phagocytosis by *Sirpa*$^{hu/hu}$ macrophages was further significantly reduced compared with that by *Sirpa*$^{NOD/NOD}$ macrophages, correlating inversely with their affinity in binding assays (Figure 1B).

Sirpa$^{hu/hu}$ macrophages have moderate affinity for mouse CD47

Although *Sirpa*$^{-/-}$ mice were reported to develop anemia or thrombocytopenia,[31,32] *Sirpa*$^{hu/hu}$ mice did not appear to have these cytopenias (data not shown). Therefore, we tested the binding affinity for mouse CD47-Fc protein in macrophages from *Sirpa*$^{W/W}$, *Sirpa*$^{NOD/NOD}$, or *Sirpa*$^{hu/hu}$ mice. As shown in Figure 1E, B6-*Sirpa*$^{NOD/NOD}$ macrophages had a strong binding affinity to mouse CD47 (Bmax, 0.80 ± 0.09) that was comparable to normal B6-*Sirpa*$^{W/W}$ mice (Bmax, 0.70 ± 0.05). Interestingly, B6-*Sirpa*$^{hu/hu}$ macrophages bound to mouse CD47 at a moderate level (Bmax, 0.29 ± 0.02), suggesting the possibility that human SIRPA derived from a full-length human *SIRPA* knock-in allele can recognize mouse CD47 to prevent phagocytosis against autologous mouse cells.

The BRGS^{human} mouse did not develop anemia or thrombocytopenia and had a long lifespan

The BRGS^{human} mouse was established by crossing the BRG mouse with the B6-*Sirpa*$^{hu/hu}$ mouse. BRGS^{human} mice were born healthy and exhibited good fertility. As shown in Figure 2A, they had normal levels of hemoglobin and platelets, unlike *Sirpa*$^{-/-}$ mice,[23] and had reduced numbers of leukocytes as a result of T, B, and NK lymphocyte depletion (Figure 2B). These phenotypes were similar to BRGS^{NOD} mice.[19] Like NSG or BRGS^{NOD} mice, BRGS^{human} mice had a median lifespan of 71 weeks without developing lymphoma, which is the major cause of death in NOD-*scid* mice or NOD-*Rag1*^{null}–based strains (Figure 2C).[7,9]

The BRGS^{human} mouse showed reconstitution of human hematopoiesis and myelopoiesis that was more efficient than the BRGS^{NOD} mouse in the bone marrow

Six- to 8-week-old BRG, BRGS^{NOD}, and BRGS^{human} mice were irradiated and transplanted with 5 × 10^3 CD34$^+$CD38$^-$ human CB cells. At 10 to 12 weeks after transplantation, human CD45$^+$ cells were not detectable in BRG mice (Figure 3A, left panel).

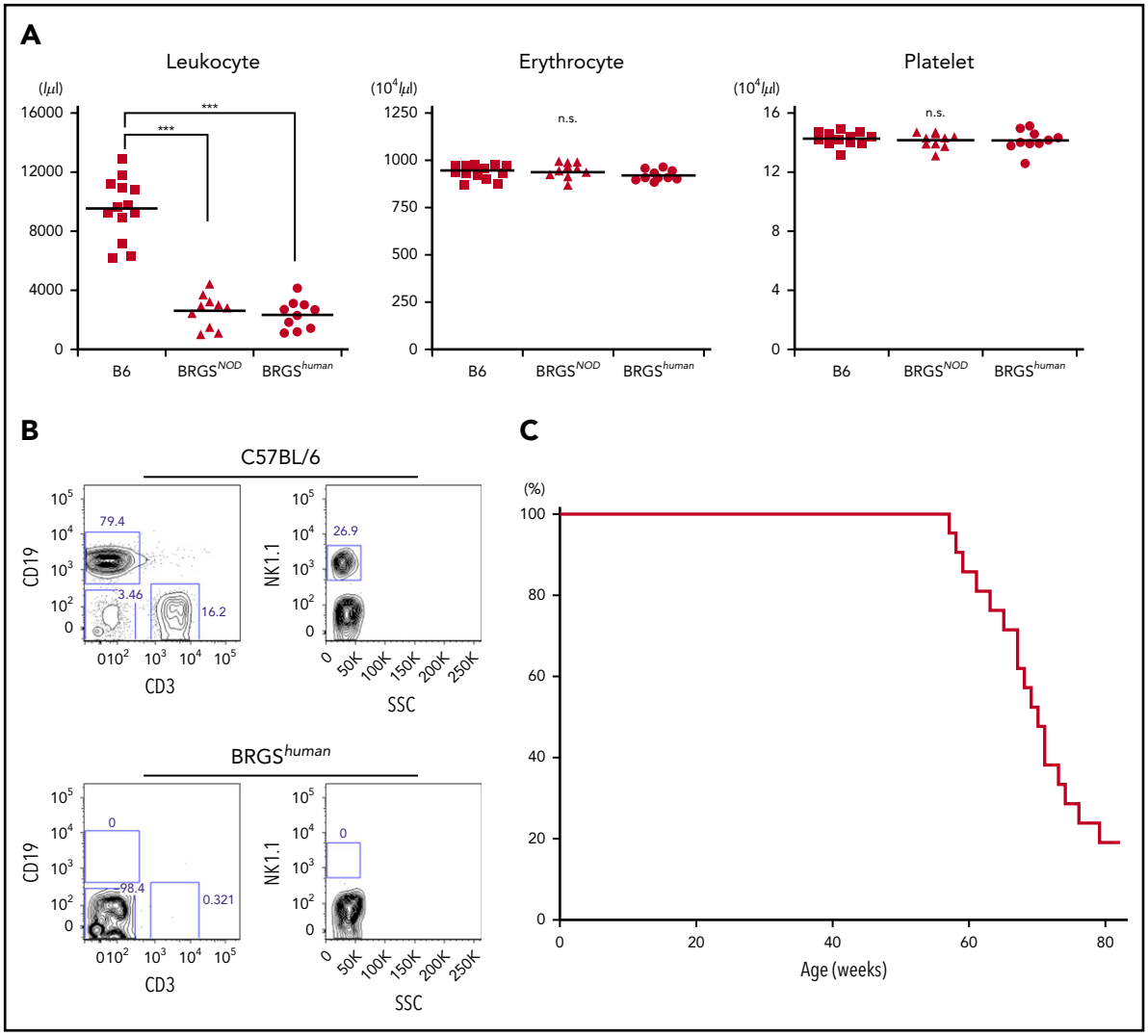

Figure 2. BRGS^{human} mice do not exhibit anemia or thrombocytopenia and have a long lifespan. (A) Frequencies of blood leukocytes, erythrocytes, and platelets in adult B6, BRGS^{NOD}, and BRGS^{human} mice. BRGS^{human} mice have leukopenia resulting from a loss of lymphocytes but have normal numbers of erythrocytes and platelets. (B) Representative flow cytometric plots of blood in B6 and BRGS^{human} mice. BRGS^{human} mice lacked T, B, and NK cells. (C) Kaplan-Meyer survival curve of BRGS^{human} mice (n = 22). ***$P < .001$.

BRGS^{NOD} and BRGS^{human} mice showed successful human hematopoietic reconstitution in the bone marrow, and the average frequency of human CD45$^+$ cells in BRGS^{human} mice was significantly higher than that of BRGS^{NOD} mice (80.9% vs 68.9%, respectively). We then analyzed the long-term reconstitution at 20 to 24 weeks after transplantation, because maintenance of human hematopoiesis for >20 weeks is dependent upon self-renewal of human HSCs in the mouse bone marrow niche.[33] As shown in Figure 3A (right panel), BRGS^{human} mice maintained a high level of human cell chimerism (mean, 55.9%) in the bone marrow, exceeding the level in BRGS^{NOD} mice (mean, 42.9%). Then, 10^6 human CD45$^+$ cells were purified from primary BRGS^{NOD} or BRGS^{human} recipients at 10 to 12 weeks after xenotransplantation, and these cells were retransplanted into irradiated adult BRGS^{NOD} mice. Eight weeks after the secondary transplantation, re-engraftment of human hematopoietic cells was observed at equivalent levels in the 2 groups (Figure 3B). These data suggest that the BRGS^{human} and BRGS^{NOD} microenvironments are able to support self-renewal of human HSCs.

Next, we performed a limiting dilution assay to quantitate the frequency of repopulating cells by injecting graded doses of CD34$^+$CD38$^-$ CB cells (10^1, 10^2, or 10^3 cells per injection) (Figure 3C). The frequency of detectable repopulating cells in the bone marrow was significantly higher in BRGS^{human} mice (1 per 32 injected cells) vs BRGS^{NOD} mice (1 per 141 injected cells).

Figure 4A shows the lineage analysis of human CD45$^+$ cells reconstituted in the bone marrow after injection of 5×10^3 CD34$^+$CD38$^-$ CB cells. The percentage of CD33$^+$ myeloid cells in BRGS^{human} mice was 22% and 26% at 10 to 12 weeks and 20 to 24 weeks after transplantation, respectively, whereas the percentage was only 9% and 13%, respectively, in BRGS^{NOD} mice, demonstrating that myeloid reconstitution was significantly better in BRGS^{human} mice (Figure 4B, top panels). As a result, the percentages of B cells were lower in BRGS^{human} mice (Figure 4B, middle panels). The majority of reconstituted B cells were CD10$^+$CD19$^+$CD20$^-$ immature B cells (supplemental Figure 4). T-cell reconstitution in the bone marrow appeared to be more efficient in BRGS^{human} mice (6%) than in BRGS^{NOD} mice (1%) at

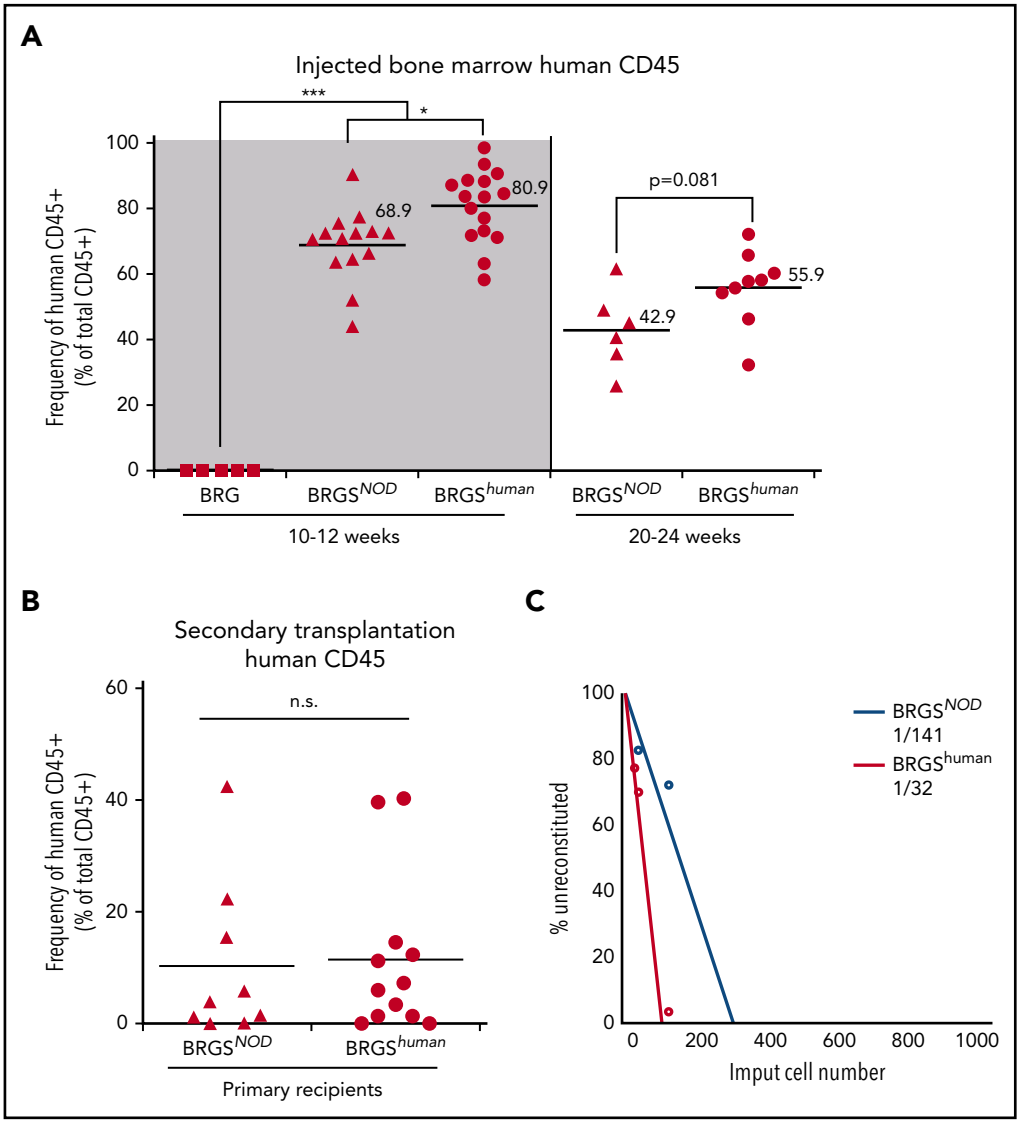

Figure 3. BRGS^{human} mice support engraftment and repopulating capability of human HSCs more efficiently than do BRGS^{NOD} mice. (A) Frequencies of human CD45$^+$ cells in the bone marrow of BRG, BRGS^{NOD}, and BRGS^{human} recipient mice injected with 5×10^3 human Lin$^-$CD34$^+$CD38$^-$ cells at 10 to 12 weeks (left panel) and at 20 to 24 weeks (right) after transplantation (n = 5-16 mice per strain). The numbers and horizontal lines indicate mean values. (B) Frequencies of human CD45$^+$ cells in the bone marrow of secondary BRGS^{NOD} recipients injected with 1×10^6 human CD45$^+$ cells purified from the bone marrow of primary BRGS^{NOD} or BRGS^{human} recipients. The horizontal lines represent mean values. (C) A limiting dilution assay was used to determine the frequencies of repopulating cells of human HSCs in BRGS^{human} mice (1 in 32 cells) and BRGS^{NOD} mice (1 in 141 cells). *$P < .05$, ***$P < .001$. n.s., not significant.

20 to 24 weeks, although the difference was not statistically significant.

Significant improvement in human hematopoiesis reconstitution in the periphery of BRGS^{human} mice

Reconstitution of human hematopoietic cells in the periphery is generally low in xenotransplantation models.[34,35] Figure 5 shows the reconstitution in the blood and the spleen in BRGS^{NOD} and BRGS^{human} mice. Compared with BRGS^{NOD} mice, peripheral reconstitution of human CD45$^+$ cells was dramatically improved in BRGS^{human} mice at 10 to 12 weeks after transplantation, and it was further improved at 20 to 24 weeks, reaching up to 22% and 42% in the blood and the spleen, respectively. Of note, the percentages of CD33$^+$ myeloid cells within CD45$^+$ cells also progressively increased in the periphery up to 32% and 17% in the blood and the spleen, respectively, at 20 to 24 weeks after transplantation.

Enhanced engraftment and growth of human cancer cells in the BRGS^{human} mouse

We wanted to test whether the BRGS^{human} mouse showed efficient engraftment of cancer cells. We transplanted 10^6 CD33$^+$CD45RA^{lo} AML cells (patients 1 and 2) or 10^6 CD34$^+$ AML cells (patient 3) purified from the bone marrow into irradiated BRGS^{NOD} and BRGS^{human} mice and serially evaluated chimerism in the blood after xenotransplantation. Clinical characteristics of patients are shown in supplemental Table 3. As shown in Figure 6, BRGS^{human} recipient mice showed accelerated leukemia reconstitution, and human CD45$^+$CD33$^+$ leukemia cell chimerisms in the blood were significantly higher than those in BRGS^{NOD} recipients 10 to 16 weeks after

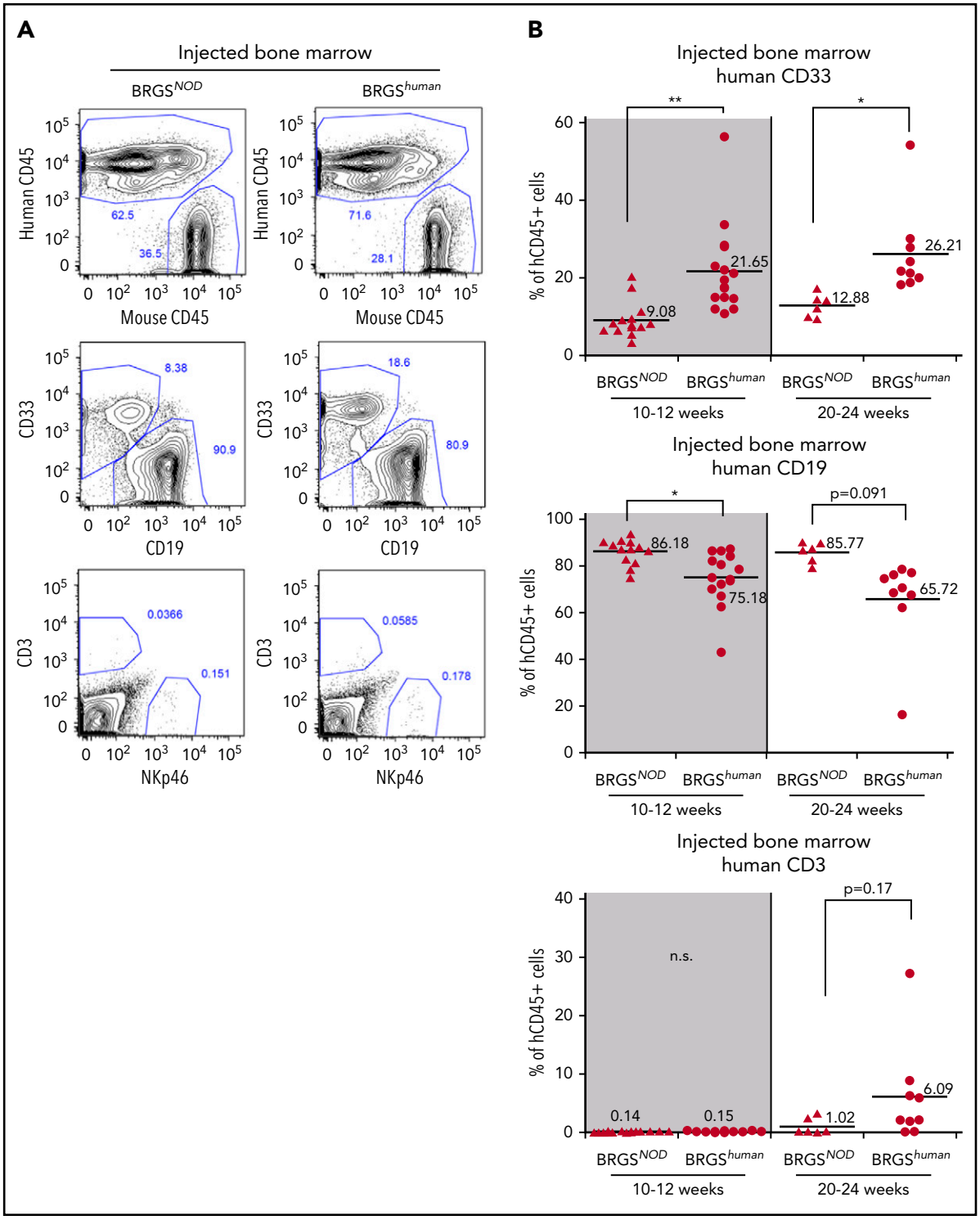

Figure 4. Human myeloid cell reconstitution is enhanced in BRGS^{human} mice. (A) Representative flow cytometric plots of reconstituted human hematopoietic cells in the bone marrow of BRGS^{NOD} or BRGS^{human} recipients. The percentages of each lineage are shown as those within the human CD45$^+$ population. Numbers indicate the percentages of gated cells. (B) Frequencies of human CD33$^+$ myeloid cells (top panels), CD19$^+$ B cells (middle panels), and CD3$^+$ T cells (bottom panels) in bone marrow at 10 to 12 weeks (left panels) and at 20 to 24 weeks (right panels) after transplantation. The numbers and horizontal lines indicate mean values. *$P < .05$, **$P < .01$. n.s., not significant.

transplantation in all 3 experiments. The chimerism of AML cells in the bone marrow was also higher in BRGS^{human} recipients at the final analysis. In the analysis of patient 3, we also transplanted AML cells into NSG mice in parallel with BRGS^{NOD} and BRGS^{human} mice. The AML cell chimerism appeared to be higher in BRGS^{human} mice than in NSG mice in the blood and the bone marrow, although the difference was not statistically significant.

The DLD-1 cell line was used to test xenotransplantation efficiency for human CRC. We transplanted 10^3 DLD-1 cells

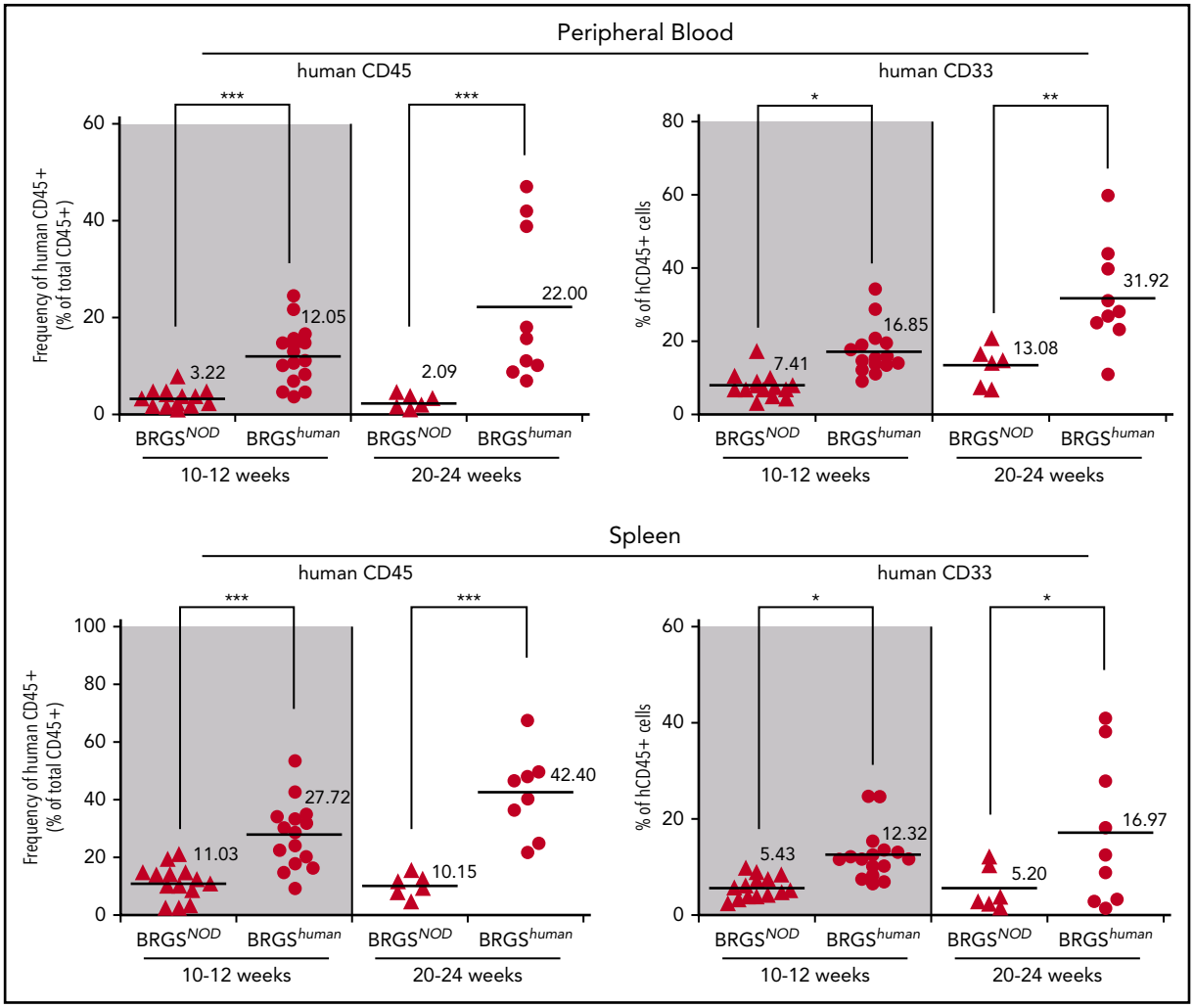

Figure 5. Human hematopoiesis reconstitution in the periphery is enhanced in BRGS^{human} mice. Proportions of human CD45$^+$ cells and CD33$^+$ myeloid cells in peripheral blood (upper panels) and spleen (lower panels) of BRGS^{NOD} and BRGS^{human} recipients. The numbers and horizontal bars indicate mean values. *$P < .05$, **$P < .01$, ***$P < .001$.

subcutaneously with Matrigel, as previously described.[30] As shown in Figure 7A, DLD-1 cells successfully engrafted, but the tumor was always bigger in BRGS^{human} recipient mice vs BRGS^{NOD} recipient mice. A limiting dilution analysis for tumor engraftment showed that the frequency of detectable tumor-initiating DLD-1 cells was 2.4-fold higher in BRGS^{human} recipient mice (Figure 7B).

We then tested xenotransplantation efficiency for primary human CRC cells. Primary tumor was obtained from patients with CRC, surgical specimens were injected into BRGS^{NOD} mice subcutaneously, and engrafted tumor cells were collected. A total of 10^5 engrafted CRC cells was subcutaneously injected into BRGS^{human} or BRGS^{NOD} mice, and secondary tumorigenesis of colon cancer cells was monitored for 10 weeks. Tumor formation was facilitated to a more significant degree in BRGS^{human} mice compared with BRGS^{NOD} mice (Figure 7C-D). These data strongly suggest that the introduction of human *SIRPA* into immunodeficient mice can provide a microenvironment suitable for engraftment and growth of human malignant hematopoiesis, as well as for CRC development.

Discussion

In establishing xenotransplantation models, deletion of lymphocytes has been achieved by introduction of the *scid* mutation in the *Prkdc* gene or disrupting key lymphoid genes, such as *Rag* and *Il2rg*. Another important factor for xenotransplantation efficiency is "macrophage tolerance" driven by the CD47-SIRPA axis, and the NOD-type SIRPA has a polymorphism that is best suited for xenotransplantation models, because it can recognize human CD47 with the highest affinity among a variety of mouse strains.[17] In this study, by directly comparing the xenotransplantation efficiency of BRGS^{human} mice with BRGS^{NOD} mice, whose efficiency was at least equal to NOD-RG mice, we showed that homozygous replacement of NOD-type mouse *Sirpa* with human *SIRPA* significantly improved the engraftment efficiency of normal human hematopoiesis, as well as of malignant blood and solid cancers.

The high efficiency of xenotransplantation in BRGS^{human} mice should be ascribed to the fact that human SIRPA has a much higher affinity for human CD47 than does NOD-type mouse SIRPA (Figure 1B). Interestingly, human SIRPA can also recognize

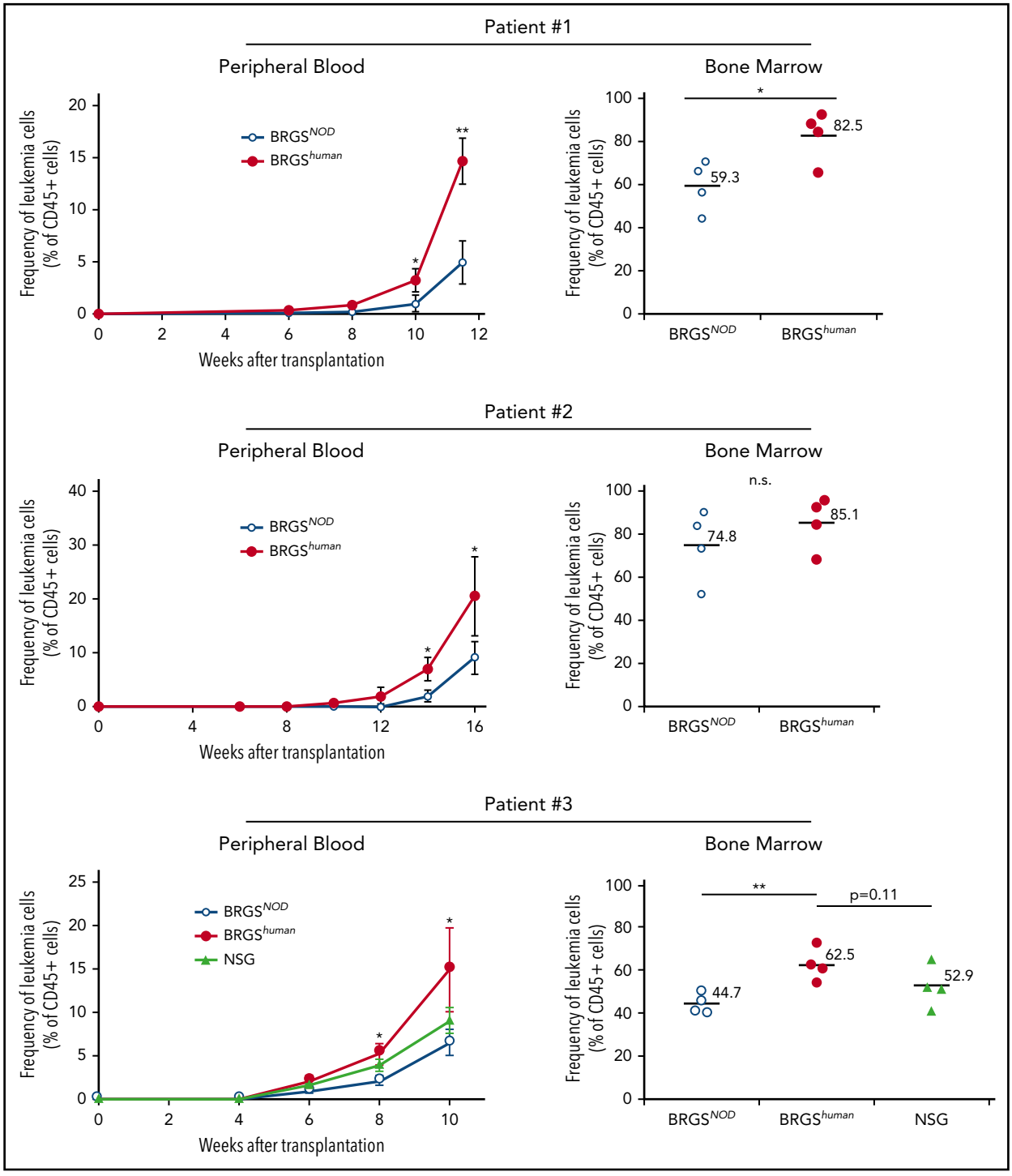

Figure 6. BRGS^{human} mice show efficient reconstitution of human AML. The kinetics of human CD45$^+$CD33$^+$ AML cells (patients 1 and 2, top and middle panels) and CD34$^+$ AML cells (patient 3; bottom panels) after transplantation into BRGS^{human}, BRGS^{NOD}, and NGS mice in the peripheral blood (left panels) and the bone marrow (right panels). The proportions of AML cells in the blood were monitored every 2 weeks, followed by the analysis of bone marrow at the final time point. In all 3 experiments, human AML cell chimerism in BRGS^{human} mice exceeded that in BRGS^{NOD} mice. *$P < .05$, **$P < .01$. n.s., not significant.

mouse CD47 (Figure 1E). *Sirpa*$^{hu/hu}$ mice and BRGS^{human} mice did not develop anemia or thrombocytopenia, probably because the engagement of mouse CD47 with human SIRPA can induce signaling at a level sufficient to keep homeostasis within the bone marrow microenvironment in BRGS^{human} mice. As a result, the BRGS^{human} mouse line is stable and has a lifespan comparable to BRGS^{NOD} mice (Figure 2C).

Moreover, the capabilities to support human hematopoiesis in BRGS^{human} mice might be better than those in previous mouse lines expressing human SIRPA. The 129.BALB-RG mouse with a transgenic BAC human *SIRPA* showed engraftment levels similar to the NSG mouse that has the NOD-type mouse SIRPA in the bone marrow, the blood, or the spleen.[26] It might be difficult to guarantee physiologically faithful expression of the BAC

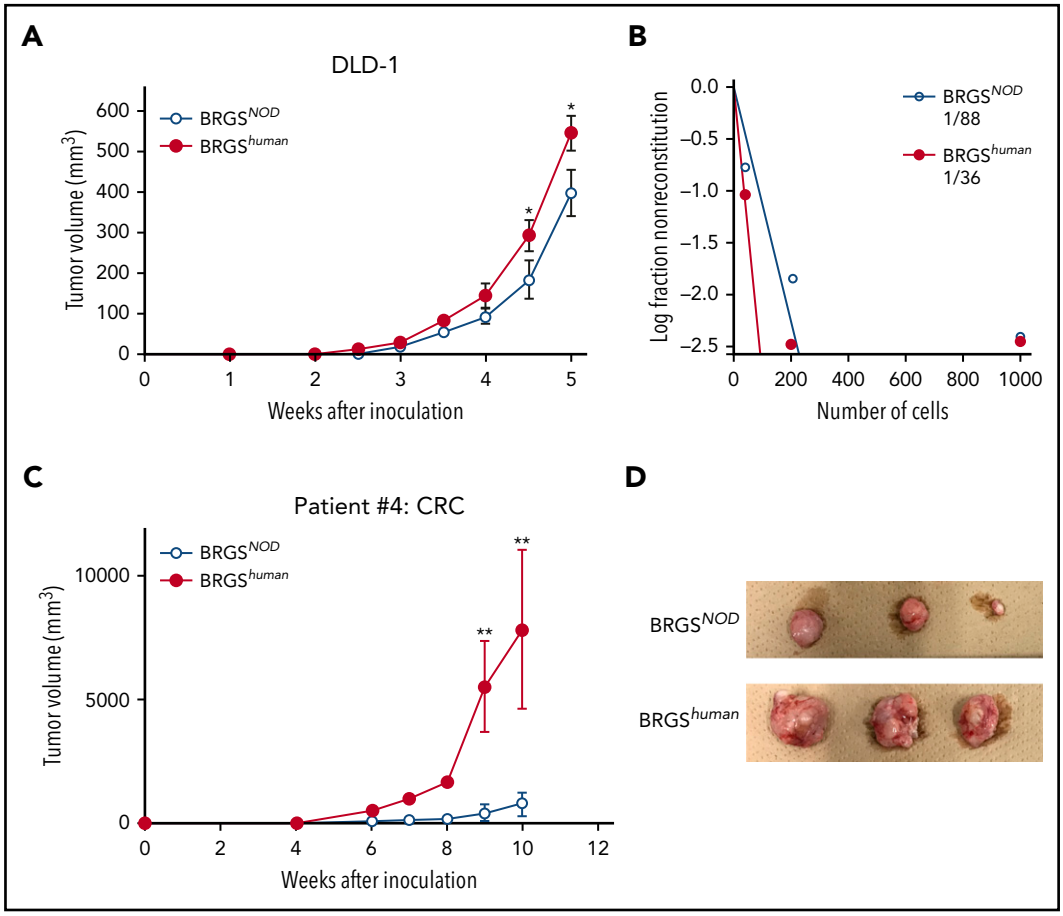

Figure 7. BRGS^{human} mice show efficient reconstitution of human solid cancer cells. (A) Tumor growth curves of DLD-1 cells. DLD-1 cells were transplanted subcutaneously into BRGS^{NOD} or BRGS^{human} mice, and tumor volume was measured every week (n = 6 each). (B) Analysis of tumor-forming capabilities of DLD-1 cells in BRGS^{NOD} and BRGS^{human} recipients using an extreme limiting dilution assay; 40, 200, or 1000 DLD-1 cells were injected subcutaneously into BRGS^{NOD} and BRGS^{human} mice (n = 6 each). Tumor formation was examined 4 weeks after inoculation. (C) Growth curves of xenograft tumors produced by patient-derived CRC cells 10 weeks after inoculation (n = 6 each). Data are mean ± standard deviation. (D) The tumor harvested from each mouse at 10 weeks after inoculation. *$P < .05$, **$P < .01$.

transgenic human SIRPA; transgenic expression of human SIRPA depends upon human SIRPA regulatory elements that are regulated by mouse intracellular components. Signaling downstream of BAC transgenic SIRPA should also be complicated in this mouse, because its macrophages coexpress endogenous mouse SIRPA.

The 129.BALB-RG strain has also been used to establish human *SIRPA* knock-in mice, whose knock-in construct was restricted to exons 2 to 4 that code for the extracellular IgV domain of human *SIRPA*.[27] Mouse and human *SIRPA* have 8 exons: exons 1 to 4 for the extracellular domain, exon 5 for the transmembrane domain, and exons 6 to 8 for the intracellular domain. The intracellular domain is mostly preserved in mice and humans. In this human *SIRPA* knock-in model that has human/mouse chimeric SIRPA, the xenotransplantation efficiency of heterozygous knock-in mice was almost equal to that of NSG mice.[27] It appears to be accurate, because the affinity of *Sirpa*$^{NOD/NOD}$ macrophages for human CD47 was similar to that of heterozygous *Sirpa*$^{hu/W}$ macrophages in our study (Figure 1B). However, homozygous knock-in mice showed significantly lower xenotransplantation efficiency compared with heterozygous mice, and the investigators speculated that hematopoietic niche formation was impaired by the lack of mouse SIRPA-CD47 signal-dependent bone and stromal cell differentiation, which was observed in SIRPA-deficient mice.[24] Because native human SIRPA can recognize mouse CD47 (Figure 1E) and BRGS^{human} mice that have homozygous full-length human *SIRPA* showed higher xenotransplantation efficiency than BRGS^{NOD} mice (Figures 3 and 4), it is possible that the chimeric SIRPA somehow lost its affinity for mouse CD47, which native human SIRPA has.

It is noteworthy that CD33^{+} myeloid cell development, as well as hematopoietic reconstitution in the periphery, was significantly improved in BRGS^{human} mice. In mouse models based on the NOD or BALB/c background, human hematopoietic reconstitution is B-cell dominant, whereas reconstitution for human myeloid lineage cells is usually limited.[12,36] Improvement of myeloid reconstitution has been reported by introducing knock-in human cytokines, including human thrombopoietin[37] and stem cell factor,[38] into NSG mice or introducing a combination of cytokines, such as macrophage colony-stimulating factor, interleukin-3, granulocyte-macrophage colony-stimulating factor, and thrombopoietin, into human BAC-SIRPA transgenic or heterozygous chimeric SIRPA knock-in mice[39-41]; this suggests that a deficiency in cross-reactivity in mouse and human cytokines causes this skewed differentiation. Significant improvement in myeloid differentiation in BRGS^{human} mice without

humanization of cytokines further suggests that physiologically appropriate CD47-SIRPA signaling is critical for human myeloid engraftment, presumably through normalization of macrophage functions in the bone marrow microenvironment[42,43] or through inhibition of macrophage engulfment or activation in the periphery.[21,44] Because the human cytokine(s) knocked-in and the homozygous full-length SIRPA^{human} knocked-in should contribute to myeloid engraftment through independent mechanisms, it might be promising to further improve engraftment by humanization of cytokines in the BRGS^{human} mouse model. It is also tempting to introduce c-Kit mutations[28,45] into BRGS^{human} mice, because BRGS^{NOD} mice with a *Kit^{Wv}* mutation exhibited highly efficient engraftment of human erythropoiesis and thrombopoiesis.[28]

Human leukemia and a variety of solid cancer cells express CD47 at a level higher than normal tissue cells to reinforce engagement of CD47 and SIRPA, as well as to escape from innate immune surveillance by macrophages.[46-48] CD47-SIRPA signaling is also required for cancer cells to survive in the xenotransplantation setting, because human cancer cells transplanted into NOD-*scid* mice were eliminated by administration of anti-CD47–blocking antibodies.[48] Therefore, significant improvement of human cancer cell engraftment in our BRGS^{human} model (Figure 7) might be due to enhanced binding of tumor CD47 and human SIRPA that evokes strong signaling to inhibit xenogeneic tumor immunity.

In summary, we generated BRGS^{human} mice with a knock-in allele of the entire human *SIRPA*. Engraftment of human CB in BRGS^{human} mice was more efficient than in BRGS^{NOD} mice in the bone marrow and in the periphery, and myeloid reconstitution was also significantly improved. The engraftment of AML cells and CRC cells was also more efficient in BRGS^{human} mice than in BRGS^{NOD} mice. These data strongly suggest that the BRGS^{human} mouse should be very useful to establish future xenogeneic transplantation assays that are more realistic for the analysis of hematopoiesis, leukemogenesis, and tumorigenesis in humans.

Acknowledgments

The authors thank Yuichiro Semba, Masayasu Hayashi, Jun Odawara, and Yasuyuki Ohkawa for purification of the CD47-Fc protein and the Japanese Red Cross Kyushu Cord Blood Bank for providing CB samples.

This work was supported in part by a Grant-in-Aid for Scientific Research (B) from Japan Society for the Promotion of Science (18H02840, K.T.), a Grant-in-Aid for Scientific Research (S) from Japan Society for the Promotion of Science (16H06391, K.A.), and a grant from the Shin-nihon Foundation of Advanced Medical Treatment Research (Y.K.)

Authorship

Contribution: F.J., T.Y., and K.T. coordinated the project, designed and performed the experiments, analyzed the data, and wrote the manuscript; A.Y., T.N., M.N., C.I., T.O., K.M., and Y.K. performed experiments; and K.K., T. Maeda, T. Miyamoto, E.B., and K.A. designed the experiments, reviewed the data, and edited the manuscript.

Conflict-of-interest disclosure: The authors declare no competing financial interests.

ORCID profiles: F.J., 0000-0003-1031-1980; M.N., 0000-0003-1049-5791; T.M., 0000-0003-4530-6460.

Correspondence: Koichi Akashi, Kyushu University Graduate School of Medical Sciences, 3-1-1 Maidashi, Higashi-ku, Fukuoka 812-8582, Japan; e-mail: akashi@med.kyushu-u.ac.jp.

Footnotes

Submitted 28 June 2019; accepted 20 February 2020; prepublished online on *Blood* First Edition 23 March 2020. DOI 10.1182/blood.2019002194.

The online version of this article contains a data supplement.

There is a *Blood* Commentary on this article in this issue.

The publication costs of this article were defrayed in part by page charge payment. Therefore, and solely to indicate this fact, this article is hereby marked "advertisement" in accordance with 18 USC section 1734.

REFERENCES

1. Goyama S, Wunderlich M, Mulloy JC. Xenograft models for normal and malignant stem cells. *Blood*. 2015;125(17):2630-2640.
2. Ishikawa F. Modeling normal and malignant human hematopoiesis in vivo through newborn NSG xenotransplantation. *Int J Hematol*. 2013;98(6):634-640.
3. Theocharides APA, Rongvaux A, Fritsch K, Flavell RA, Manz MG. Humanized hematolymphoid system mice. *Haematologica*. 2016;101(1):5-19.
4. Hidalgo M, Amant F, Biankin AV, et al. Patient-derived xenograft models: an emerging platform for translational cancer research. *Cancer Discov*. 2014;4(9):998-1013.
5. Greiner DL, Hesselton RA, Shultz LD. SCID mouse models of human stem cell engraftment. *Stem Cells*. 1998;16(3):166-177.
6. McCune JM, Namikawa R, Kaneshima H, Shultz LD, Lieberman M, Weissman IL. The SCID-hu mouse: murine model for the analysis of human hematolymphoid differentiation and function. *Science*. 1988;241(4873):1632-1639.
7. Shultz LD, Schweitzer PA, Christianson SW, et al. Multiple defects in innate and adaptive immunologic function in NOD/LtSz-scid mice. *J Immunol*. 1995;154(1):180-191.
8. Goldman JP, Blundell MP, Lopes L, Kinnon C, Di Santo JP, Thrasher AJ. Enhanced human cell engraftment in mice deficient in RAG2 and the common cytokine receptor γ chain. *Br J Haematol*. 1998;103(2):335-342.
9. Shultz LD, Banuelos S, Lyons B, et al. NOD/LtSz-Rag1nullPfpnull mice: a new model system with increased levels of human peripheral leukocyte and hematopoietic stem-cell engraftment. *Transplantation*. 2003;76(7):1036-1042.
10. Shultz LD, Lang PA, Christianson SW, et al. NOD/LtSz-Rag1null mice: an immunodeficient and radioresistant model for engraftment of human hematolymphoid cells, HIV infection, and adoptive transfer of NOD mouse diabetogenic T cells. *J Immunol*. 2000;164(5):2496-2507.
11. Ishikawa F, Yasukawa M, Lyons B, et al. Development of functional human blood and immune systems in NOD/SCID/IL2 receptor γ chain(null) mice. *Blood*. 2005;106(5):1565-1573.
12. Ito M, Hiramatsu H, Kobayashi K, et al. NOD/SCID/γ(c)(null) mouse: an excellent recipient mouse model for engraftment of human cells. *Blood*. 2002;100(9):3175-3182.
13. Shultz LD, Lyons BL, Burzenski LM, et al. Human lymphoid and myeloid cell development in NOD/LtSz-scid IL2R γ null mice engrafted with mobilized human hemopoietic stem cells. *J Immunol*. 2005;174(10):6477-6489.
14. Brehm MA, Cuthbert A, Yang C, et al. Parameters for establishing humanized mouse models to study human immunity: analysis of human hematopoietic stem cell engraftment in three immunodeficient strains of mice bearing the IL2rgamma(null) mutation. *Clin Immunol*. 2010;135(1):84-98.
15. Pearson T, Shultz LD, Miller D, et al. Non-obese diabetic-recombination activating gene-1 (NOD-Rag1 null) interleukin (IL)-2 receptor common gamma chain (IL2r gamma null) null mice: a radioresistant model for

human lymphohaematopoietic engraftment. *Clin Exp Immunol*. 2008;154(2):270-284.

16. Traggiai E, Chicha L, Mazzucchelli L, et al. Development of a human adaptive immune system in cord blood cell-transplanted mice. *Science*. 2004;304(5667):104-107.

17. Iwamoto C, Takenaka K, Urata S, et al. The BALB/c-specific polymorphic SIRPA enhances its affinity for human CD47, inhibiting phagocytosis against human cells to promote xenogeneic engraftment. *Exp Hematol*. 2014; 42(3):163-171.e1.

18. Takenaka K, Prasolava TK, Wang JCY, et al. Polymorphism in Sirpa modulates engraftment of human hematopoietic stem cells. *Nat Immunol*. 2007;8(12):1313-1323.

19. Yamauchi T, Takenaka K, Urata S, et al. Polymorphic Sirpa is the genetic determinant for NOD-based mouse lines to achieve efficient human cell engraftment. *Blood*. 2013; 121(8):1316-1325.

20. Matozaki T, Murata Y, Okazawa H, Ohnishi H. Functions and molecular mechanisms of the CD47-SIRPalpha signalling pathway. *Trends Cell Biol*. 2009;19(2):72-80.

21. Kuriyama T, Takenaka K, Kohno K, et al. Engulfment of hematopoietic stem cells caused by down-regulation of CD47 is critical in the pathogenesis of hemophagocytic lymphohistiocytosis. *Blood*. 2012;120(19): 4058-4067.

22. Oldenborg P-A, Zheleznyak A, Fang Y-F, Lagenaur CF, Gresham HD, Lindberg FP. Role of CD47 as a marker of self on red blood cells. *Science*. 2000;288(5473):2051-2054.

23. Yamao T, Noguchi T, Takeuchi O, et al. Negative regulation of platelet clearance and of the macrophage phagocytic response by the transmembrane glycoprotein SHPS-1. *J Biol Chem*. 2002;277(42):39833-39839.

24. Koskinen C, Persson E, Baldock P, et al. Lack of CD47 impairs bone cell differentiation and results in an osteopenic phenotype in vivo due to impaired signal regulatory protein α (SIRPα) signaling. *J Biol Chem*. 2013;288(41): 29333-29344.

25. Kwong LS, Brown MH, Barclay AN, Hatherley D. Signal-regulatory protein α from the NOD mouse binds human CD47 with an exceptionally high affinity-- implications for engraftment of human cells. *Immunology*. 2014; 143(1):61-67.

26. Strowig T, Rongvaux A, Rathinam C, et al. Transgenic expression of human signal regulatory protein alpha in Rag2-/-γ(c)-/- mice improves engraftment of human hematopoietic cells in humanized mice. *Proc Natl Acad Sci USA*. 2011;108(32):13218-13223.

27. Herndler-Brandstetter D, Shan L, Yao Y, et al. Humanized mouse model supports development, function, and tissue residency of human natural killer cells. *Proc Natl Acad Sci USA*. 2017;114(45):E9626-E9634.

28. Yurino A, Takenaka K, Yamauchi T, et al. Enhanced reconstitution of human erythropoiesis and thrombopoiesis in an immunodeficient mouse model with Kit(Wv) mutations. *Stem Cell Reports*. 2016;7(3): 425-438.

29. McKenzie JL, Gan OI, Doedens M, Dick JE. Human short-term repopulating stem cells are efficiently detected following intrafemoral transplantation into NOD/SCID recipients depleted of CD122+ cells. *Blood*. 2005; 106(4):1259-1261.

30. Tamura S, Isobe T, Ariyama H, et al. E-cadherin regulates proliferation of colorectal cancer stem cells through NANOG. *Oncol Rep*. 2018;40(2):693-703.

31. Inagaki K, Yamao T, Noguchi T, et al. SHPS-1 regulates integrin-mediated cytoskeletal reorganization and cell motility. *EMBO J*. 2000; 19(24):6721-6731.

32. Okazawa H, Motegi S, Ohyama N, et al. Negative regulation of phagocytosis in macrophages by the CD47-SHPS-1 system. *J Immunol*. 2005;174(4):2004-2011.

33. Notta F, Doulatov S, Laurenti E, Poeppl A, Jurisica I, Dick JE. Isolation of single human hematopoietic stem cells capable of long-term multilineage engraftment. *Science*. 2011;333(6039):218-221.

34. Futrega K, Lott WB, Doran MR. Direct bone marrow HSC transplantation enhances local engraftment at the expense of systemic engraftment in NSG mice. *Sci Rep*. 2016;6(1): 23886.

35. Beyer AI, Muench MO. Comparison of human hematopoietic reconstitution in different strains of immunodeficient mice. *Stem Cells Dev*. 2017;26(2):102-112.

36. Doulatov S, Notta F, Laurenti E, Dick JE. Hematopoiesis: a human perspective. *Cell Stem Cell*. 2012;10(2):120-136.

37. Rongvaux A, Willinger T, Takizawa H, et al. Human thrombopoietin knockin mice efficiently support human hematopoiesis in vivo. *Proc Natl Acad Sci USA*. 2011;108(6): 2378-2383.

38. Takagi S, Saito Y, Hijikata A, et al. Membrane-bound human SCF/KL promotes in vivo human hematopoietic engraftment and myeloid differentiation. *Blood*. 2012;119(12): 2768-2777.

39. Rongvaux A, Willinger T, Martinek J, et al. Development and function of human innate immune cells in a humanized mouse model [published correction appears in *Nat Biotechnol*. 2017;35(12):1211]. *Nat Biotechnol*. 2014;32(4):364-372.

40. Deng K, Pertea M, Rongvaux A, et al. Broad CTL response is required to clear latent HIV-1 due to dominance of escape mutations. *Nature*. 2015;517(7534):381-385.

41. Song Y, Rongvaux A, Taylor A, et al. A highly efficient and faithful MDS patient-derived xenotransplantation model for pre-clinical studies. *Nat Commun*. 2019;10(1):366.

42. Chow A, Lucas D, Hidalgo A, et al. Bone marrow CD169+ macrophages promote the retention of hematopoietic stem and progenitor cells in the mesenchymal stem cell niche. *J Exp Med*. 2011;208(2):261-271.

43. Ehninger A, Trumpp A. The bone marrow stem cell niche grows up: mesenchymal stem cells and macrophages move in. *J Exp Med*. 2011;208(3):421-428.

44. Tsai RK, Discher DE. Inhibition of "self" engulfment through deactivation of myosin-II at the phagocytic synapse between human cells. *J Cell Biol*. 2008;180(5):989-1003.

45. Cosgun KN, Rahmig S, Mende N, et al. Kit regulates HSC engraftment across the human-mouse species barrier. *Cell Stem Cell*. 2014; 15(2):227-238.

46. Jaiswal S, Jamieson CHM, Pang WW, et al. CD47 is upregulated on circulating hematopoietic stem cells and leukemia cells to avoid phagocytosis. *Cell*. 2009;138(2):271-285.

47. Chao MP, Weissman IL, Majeti R. The CD47-SIRPα pathway in cancer immune evasion and potential therapeutic implications. *Curr Opin Immunol*. 2012;24(2):225-232.

48. Majeti R, Chao MP, Alizadeh AA, et al. CD47 is an adverse prognostic factor and therapeutic antibody target on human acute myeloid leukemia stem cells. *Cell*. 2009;138(2): 286-299.